ARTICLE

Induced Self-Assembly and Förster Resonance Energy Transfer Studies of Alkynylplatinum(II) Terpyridine Complex Through Interaction With Water-Soluble Poly(phenylene ethynylene sulfonate) and the Proof-of-Principle Demonstration of this Two-Component Ensemble for Selective Label-Free Detection of Human Serum Albumin

Clive Yik-Sham Chung and Vivian Wing-Wah Yam*

Institute of Molecular Functional Materials (Areas of Excellence Scheme, University Grants Committee (Hong Kong)) and Department of Chemistry, The University of Hong Kong, Pokfulam Road, Hong Kong, P.R. China

Ⓢ *Supporting Information*

ABSTRACT: The interaction of conjugated polyelectrolyte, PPE-SO$_3^-$, with platinum(II) complexes, [Pt(tpy)(C≡CC$_6$H$_4$−CH$_2$NMe$_3$-4)](OTf)$_2$ (**1**) and [Pt(tpy)(C≡C−CH$_2$NMe$_3$)]-(OTf)$_2$ (**2**), has been studied by UV−vis, and steady-state and time-resolved emission spectroscopy. A unique FRET from PPE-SO$_3^-$ to the aggregated complex **1** on the polymer chain with Pt···Pt interaction has been demonstrated, resulting in the growth of triplet metal-metal-to-ligand charge transfer (^{3}MMLCT) emission in the near-infrared (NIR) region. This two-component ensemble has been employed in a "proof-of-principle" concept for the sensitive and selective label-free detection of human serum albumin (HSA) by the emission spectral changes in the visible and in the NIR region. The spectral changes have been ascribed to the disassembly of the polymer−metal complex aggregates upon the binding of PPE-SO$_3^-$ to HSA, which is rich in arginine residues and hydrophobic patches, leading to the decrease in FRET from PPE-SO$_3^-$ to the aggregated platinum(II) complex. The ensemble is found to have high selectivity toward HSA over a number of polyelectrolytes, proteins and small amino acids. This has been suggested to be a result of the extra stabilization gained from the Pt···Pt and $\pi-\pi$ interactions in addition to the electrostatic and hydrophobic interactions found in the polymer−metal complex aggregates.
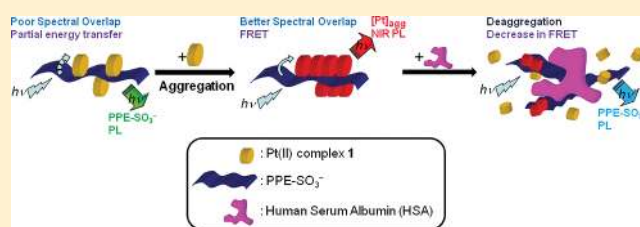
Square-planar platinum(II) polypyridyl complexes, with a strong tendency toward the formation of highly ordered extended linear chains or oligomeric structures in the solid state,[1] have attracted much attention due to their rich spectroscopic properties.[1−6] A particular class of platinum(II) complexes that has attracted long-standing interest is the alkynylplatinum-(II) terpyridine complexes, in which their d^8−d^8 metal−metal interaction and the $\pi-\pi$ interaction of the terpyridine ligands have led to the observation of interesting spectroscopic and luminescence properties.[4] Recently, our group reported the self-assembly of terpyridylplatinum(II) complexes induced by polyelectrolytes in aqueous media with remarkable UV−vis and near-infrared (NIR) emission spectral changes,[4a,d] and extended the work to detect biomolecules[4c,e−g] and their related conformational changes,[4c,e,f] such as G-quadruplex formation,[4e] as well as to probe the activities of some important biological enzymes.[4e−g]

Conjugated polyelectrolytes (CPEs) are π-conjugated polymers that feature strong absorption and fluorescence and have been extensively studied.[7−11] Interactions of CPEs in aqueous solution with metal ions, organic ions, biomolecules, and biopolymers would result in significant changes in emissions with high sensitivity.[7d−n,8b,8c,9b−e,10,11] This has been explained by the enhanced static quenching through extremely rapid exciton diffusion along the CPE chain to the quencher,[7d−n,9b−e] which was described as amplified quenching or "molecular wire effect".[7a] In addition, Förster resonance energy transfer (FRET) from the excited CPE to the quencher, which acts as an energy acceptor, plays an important role in some systems.[7k,8a−c,9e] As the efficiency of FRET strongly depends on the distance between the donor and the acceptor and their orientations,[12] FRET study can provide valuable information on the interactions between the donor and acceptor, as well as any changes of the interactions under external perturbations. However, FRET studies of CPEs have been relatively less explored,[7k,8a−c,9e] compared to the studies of CPEs with amplified quenching.[7d−n,9b−e]

Human serum albumin (HSA) is the most abundant protein in the blood plasma and serves several important biological

Scheme 1

1   2   PPE-SO$_3^-$Na$^+$
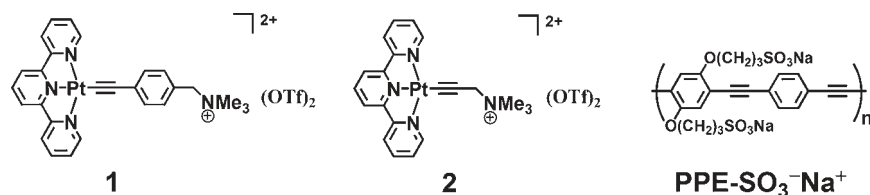
functions, such as regulation of the osmotic pressure of the blood compartment and transportation of various endogenous and exogenous substances through its role as a physiological carrier.[13] A low level of HSA in the blood plasma, which is called hypoproteinemia, would be a sign for liver failure, cirrhosis, and chronic hepatitis.[14] On the other hand, the presence of an excess amount of HSA in urine is called microalbuminuria, which is an early sign of incipient renal disease and may result in diabetes and hypertension.[15] Therefore, the detection of the concentration of HSA in blood plasma and urine has a great clinical importance. Currently, the detections by fluorescence probes[16] are generally poor in selectivity and stability,[16b−e] and their emissions in the visible region may be interfered by the fluorescence of other proteins in the biological samples.[16] As a result, the search for new luminescence assay methods with spectral changes in a spectral region other than the visible region, such as in the NIR region, may allow a rapid, selective and sensitive detection of HSA for the development of a new screening method for patients.

In view of the fact that polyelectrolytes have been reported to induce the self-assembly of alkynylplatinum(II) terpyridine complexes, it is believed that CPEs would induce the aggregation of platinum(II) moieties, leading to metal−metal and/or $\pi-\pi$ interaction with remarkable UV−vis and emission spectral changes. More importantly, as the emission wavelengths of CPEs are found to occur in a region similar to the absorption wavelength region of the alkynylplatinum(II) terpyridine complexes, FRET from the non-innocent CPEs to the aggregated metal complexes, which has not yet been reported so far, would be possible upon a judicious choice of CPEs that show emission bands that would overlap with the absorption spectrum of the alkynylplatinum(II) terpyridine system. This may result in interesting spectral changes related to FRET processes and the development of a new strategy in modulating FRET processes. Herein we report the synthesis, photophysical and FRET study of the two-component platinum(II) complex−CPE ensemble, and demonstrate the extension of the work to a "proof-of-principle" concept for the sensing of HSA through a modulation of the FRET properties and the assembly of platinum(II) complexes.

■ RESULTS AND DISCUSSION

The electronic absorption spectra of [Pt(tpy)(C≡CC$_6$H$_4$−CH$_2$NMe$_3$-4)](OTf)$_2$ (1) and poly(phenylene ethynylene) with sulfonate groups in the side chains (PPE-SO$_3^-$) (Scheme 1) in an aqueous buffer solution (30 mM Tris-HCl, 30 mM NaCl, pH 9.0) are shown in Figure 1a. The concentration of sulfonate groups in PPE-SO$_3^-$ (PE-SO$_3^-$) was 45 μM. According to the previous spectroscopic studies on poly(phenylene ethynylene),[7] the absorption bands of PPE-SO$_3^-$ with peak maxima at 336 and 435 nm are due to short- and long-axis polarized $\pi \rightarrow \pi^*$ transitions. On the other hand, the absorption spectrum of 1 shows an

absorption band centered at 340 nm and a lower-energy band centered at 417 nm. The high-energy absorption has been tentatively assigned as intraligand $\pi \rightarrow \pi^*$ transitions of the terpyridine and alkynyl ligand, whereas the lower-energy absorption has been assigned as dπ(Pt)$\rightarrow \pi^*$(tpy) metal-to-ligand charge transfer (MLCT) and alkynyl-to-terpyridine ligand-to-ligand charge transfer (LLCT) transitions typical of platinum(II) terpyridine complexes.[3,4]

Upon addition of 1 to an aqueous solution of PPE-SO$_3^-$, red shifts of the absorption bands centered at 336 and 435 nm to 350 and 448 nm, respectively, with a well-defined isosbestic point at 362 nm were observed (Figure 1b). Since 1 is known to absorb at ∼340 and 417 nm, this may contribute toward the observed red shifts. In addition, as 1 is positively charged and has been reported to undergo self-assembly to form aggregates in the presence of anionic polyelectrolytes by metal−metal and/or $\pi-\pi$ interactions absorbing at ∼490 and 570 nm,[4a,d,g] it is likely that 1 would aggregate on PPE-SO$_3^-$ and the absorption of the aggregates of 1 would contribute toward the red shifts. Furthermore, the formation of polymer aggregates induced by 1 presumably through electrostatic and $\pi-\pi$ interactions can also lead to the observed spectral changes, as similar red shifts in the absorption bands of PPE-SO$_3^-$ have been reported in the study of PPE-SO$_3^-$ with cyanine dyes.[7k] On the other hand, converse titration of 1 with increasing concentrations of PPE-SO$_3^-$ shows an isosbestic point at 295 nm and a growth of the absorptions at ∼340 and 417 nm with red shifts to ∼346 and 462 nm respectively at 45 μM of both PE-SO$_3^-$ and 1 (Figure 1c). These again suggest the possibility of the formation of polymer−metal complex aggregates, which has been further investigated by resonance light scattering (RLS), emission and time-resolved emission spectroscopic studies.

The emission spectra of PPE-SO$_3^-$ with different concentrations of 1 have been recorded upon excitation at the isosbestic wavelength of 362 nm (Figure 2). In the absence of 1, an emission band centered at 535 nm was observed, which is due to the $^1\pi-\pi^*$ fluorescence of PPE-SO$_3^-$ in aqueous solution typical of those reported in the literature.[7d,e,g−k] The intensity of this band has been found to drop drastically with an increasing concentration of 1, with the emergence of a new emission band centered at ∼795 nm as the concentration of 1 increases above 15 μM. According to the previous spectroscopic work on alkynylplatinum(II) terpyridine complexes,[4] the new emission band is tentatively assigned as triplet metal-metal-to-ligand charge transfer (^{3}MMLCT) emission through metal−metal and/or $\pi-\pi$ interactions. A further increase in the concentration of 1 to 45 μM would lead to a further drop in the emission intensity of PPE-SO$_3^-$ to only ∼1.5% of the emission intensity without 1, and a significant growth (∼18-fold) of the ^{3}MMLCT emission in the NIR region. The quenching of the PPE-SO$_3^-$ fluorescence by 1 has been investigated by Stern−Volmer experiments and the Stern−Volmer plot is shown in Figure 3.
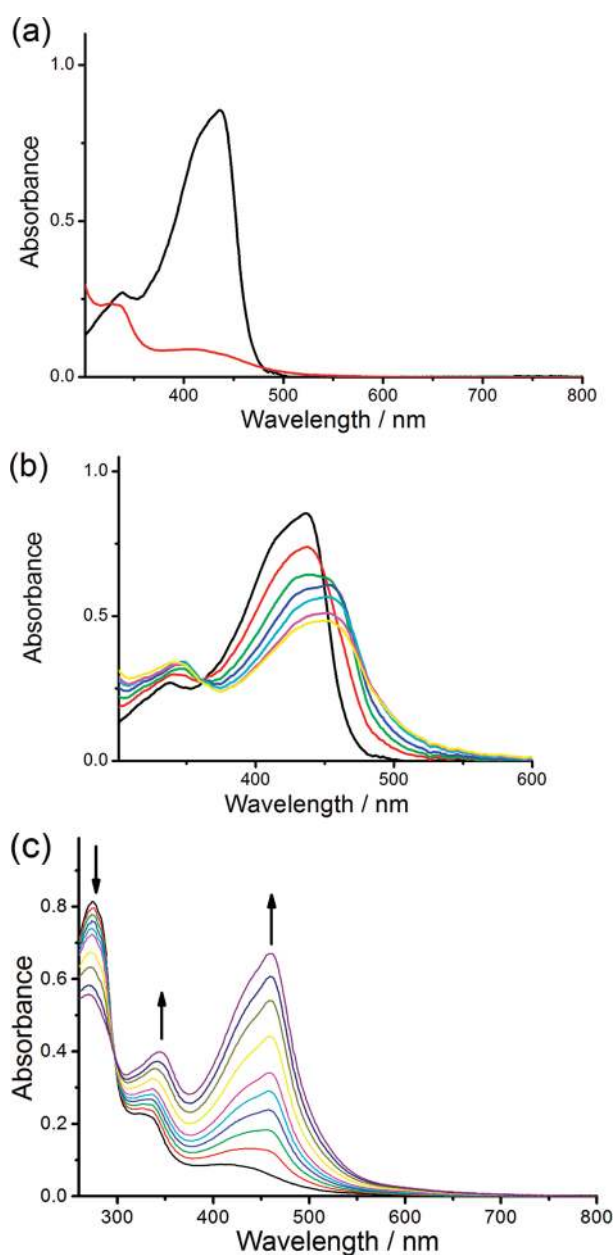
Figure 1. (a) Electronic absorption spectra of (black) PPE-SO$_3^-$ and (red) complex **1** in an aqueous buffer solution (30 mM Tris-HCl, 30 mM NaCl, pH 9.0). Concentration of **1** and sulfonate groups in PPE-SO$_3^-$ (PE-SO$_3^-$) were both 45 μM. (b) Electronic absorption spectral changes of PPE-SO$_3^-$ in the aqueous buffer solution with an increasing concentration of **1**. Concentration of PE-SO$_3^-$ and **1** were 45 μM and (black) 0 μM, (red) 7.5 μM, (green) 15 μM, (blue) 22.5 μM, (cyan) 30 μM, (magenta) 37.5 μM, (yellow) 45 μM respectively. (c) Electronic absorption spectral changes of **1** in aqueous buffer solution with an increasing concentration of PPE-SO$_3^-$. Concentration of **1** and PE-SO$_3^-$ were 45 μM and (black) 0 μM, (red) 3 μM, (green) 6 μM, (blue) 9 μM, (cyan) 12 μM, (magenta) 15 μM, (yellow) 22.5 μM, (dark yellow) 30 μM, (navy) 37.5 μM and (purple) 45 μM respectively.

The plot is found to deviate from linearity with an upward curvature and the K_{SV} value is found to increase with increasing concentration of **1** (Table 1), suggesting that the fluorescence quenching of PPE-SO$_3^-$ by **1** is more effective at higher concentrations of **1**.
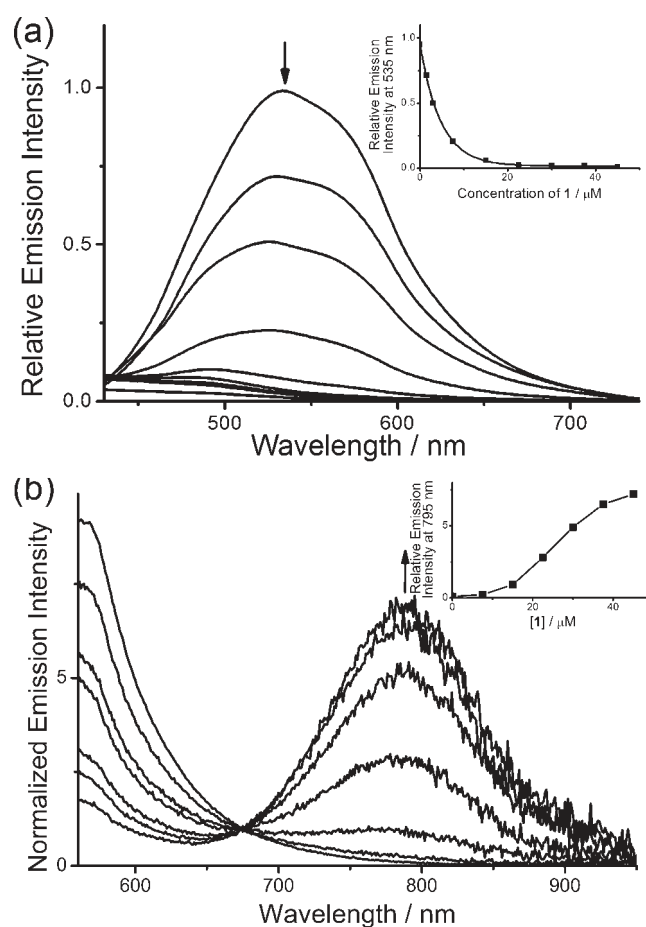
Figure 2. Emission spectral changes of PPE-SO$_3^-$ in aqueous buffer solution (30 mM Tris-HCl, 30 mM NaCl, pH 9.0) with an increasing concentration of **1** in the range of (a) 430−700 nm and (b) 560−920 nm with normalization at 674 nm. Concentration of PE-SO$_3^-$ was 45 μM. Inset: Plot of relative emission intensity at 535 and 795 nm versus concentration of **1**.

In addition, the converse titration of **1** with increasing concentrations of PPE-SO$_3^-$ would result in emission spectral changes too, as shown in Figure S1 in Supporting Information (SI). In the absence of PPE-SO$_3^-$, an emission centered at ∼633 nm is derived from an excited state of ^{3}MLCT/^{3}LLCT origin.[3,4] At 3 μM PE-SO$_3^-$, there was a diminishment of the emission intensity at 633 nm with a concomitant growth of an emission band at 795 nm, which is ascribed as ^{3}MMLCT emission originating from metal−metal and/or $\pi-\pi$ interactions typical of alkynylplatinum-(II) terpyridine complexes.[4] With increasing concentration of PE-SO$_3^-$ up to 45 μM, the ^{3}MMLCT emission was found to increase in intensity while no fluorescence from PPE-SO$_3^-$ was observed. However, further increase in the concentration of PE-SO$_3^-$ (45−75 μM) would lead to a significant drop in ^{3}MMLCT emission, while the PPE-SO$_3^-$ fluorescence at ∼513 nm was found to show an increase in intensity.

In order to have a better understanding of the quenching of PPE-SO$_3^-$ by **1**, time-resolved emission study of PPE-SO$_3^-$ in the aqueous buffer solution (30 mM Tris-HCl, 30 mM NaCl, pH 9.0) has been carried out in the presence of different concentrations of **1** (Figure 4). In the absence of **1**, the fluorescence life-times of PPE-SO$_3^-$ are found to be 1.64 and 7.48 ns (Table 1), comparable to those reported in the literature.[7d] The biexponential
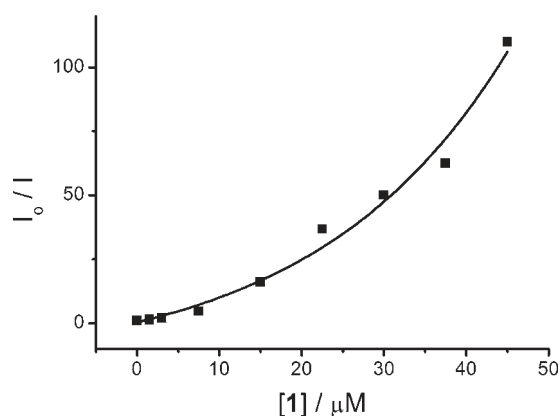
Figure 3. Stern–Volmer plot for the quenching of PPE-SO$_3^-$ by **1** in aqueous buffer solution (30 mM Tris-HCl, 30 mM NaCl, pH 9.0). Concentration of PE-SO$_3^-$ was 45 μM. I_0 and I are the emission intensity at 535 nm without **1** and with different concentrations of **1**, respectively.

Figure 4. Time-resolved emission decay of PPE-SO$_3^-$ in aqueous buffer solution (30 mM Tris-HCl, 30 mM NaCl, pH 9.0) with the concentration of **1** equal to (black) 0 μM, (red) 7.5 μM, (green) 15 μM, (blue) 22.5 μM, (cyan) 30 μM, (magenta) 37.5 μM and (yellow) 45 μM. Concentration of PE-SO$_3^-$ was 45 μM. Excitation was at 371 nm and emission signals were monitored at 535 nm. The prompt signal is shown in black squares without any line fitting.
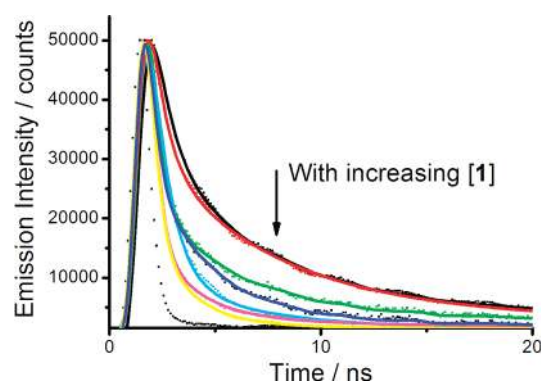
Table 1. Parameters Obtained from Steady-State Emission Spectra and Time-Resolved Emission Spectra of PPE-SO$_3^-$ in Aqueous Buffer Solution (30 mM Tris-HCl, 30 mM NaCl, pH 9.0) with Different Concentrations of 1^a

[**1**]/μM	τ_1/ns	τ_2/ns	$K_{SV}/10^5$ M^{-1} s^{-1}
0	1.64	7.48	
7.5	1.52	7.08	4.84
15	1.07	4.74	10.05
22.5	0.88	4.05	15.89
30	0.74	3.54	16.33
37.5	0.70	3.10	16.40
45	0.64	2.83	24.20

^{a} Concentration of PE-SO$_3^-$ was 45 μM. τ_1 and τ_2 are the lifetimes of the biexponential decay. K_{SV} is the Stern–Volmer quenching constant obtained from the steady-state emission measurement.

fluorescence decay could be ascribed to the formation of polymer aggregates in the aqueous buffer solution.[7d,e,g–k] At 7.5 μM of **1**, both the lifetimes, τ_1 and τ_2, are slightly shortened, while the decrease in τ_1 and τ_2 are found to be more significant at 15 μM of **1**. After such a significant decrease, an increase in the concentration of **1** has led to a further decrease in τ_1 and τ_2 values but to a smaller extent than that observed at 15 μM of **1** (Table 1).

As the fluorescence quenching is likely to be linked to the aggregation between PPE-SO$_3^-$ and **1**, RLS was performed by the titration of the polymer with **1** (Figure S2 in SI). Although PPE-SO$_3^-$ in buffer solution is known to show fluorescence at 430–700 nm, the emission has been found to be decreased significantly with increasing concentration of **1** (Figure 2a). However, in the RLS spectra, the maximum was found to show an increase in intensity with increasing concentration of **1**, suggesting that there is enhanced light scattering from the aggregates, typical of aggregate formation as reported in the literature.[17] The RLS spectrum of PPE-SO$_3^-$ shows a maximum at ~495 nm, indicative of PPE-SO$_3^-$ aggregate formation in buffer solution. The shoulder at ~555 nm is likely due to the scattering of PPE-SO$_3^-$ fluorescence as its intensity is found to decrease significantly with increasing concentrations of **1**. At 7.5 μM of **1**, the

growth of light scattering at 495 nm suggests that there is enhanced aggregation of PPE-SO$_3^-$ in the presence of **1**. In view of the absence of ^{3}MMLCT emission and thus the lack of significant self-aggregation of complex **1** with Pt···Pt and/or $\pi-\pi$ interactions at [**1**] = 7.5 μM (Figure 2b), the enhanced light scattering is ascribed to the aggregation of PPE-SO$_3^-$ by **1**, presumably through electrostatic and $\pi-\pi$ interactions. At 15 μM of **1**, apart from an increase in the light scattering at 495 nm corresponding to enhanced PPE-SO$_3^-$ aggregate formation, a new maximum at ~545 nm is found, which could be ascribed to the enhanced scattering resulting from aggregates of **1**, with Pt···Pt and/or $\pi-\pi$ interactions, on the anionic PPE-SO$_3^-$ chain through electrostatic interaction. The self-assembly and aggregation of **1** could further be supported by the steady-state emission measurements at 15 μM of **1** where ^{3}MMLCT emission at ~795 nm is found (Figure 2b). At higher concentrations of **1** (30 and 45 μM), the RLS spectra show a drop in the maximum at 495 nm with the concomitant growth of the peak at 545 nm, attributed to the increased aggregation of **1** on PPE-SO$_3^-$ and the formation of polymer–metal complex aggregates that lead to the obvious red shifts at ~340 and 417 nm in the UV–vis absorption spectra (Figure 1b).

With the formation of polymer–metal complex aggregates as suggested by RLS spectra, the mechanism for the quenching of PPE-SO$_3^-$ fluorescence and the emission spectral changes observed in the steady-state and time-resolved emission measurements at different concentrations of **1** may be interpreted as follows. At 7.5 μM of **1**, the K_{SV} value is found to be 4.84 × 10^5 M^{-1} s^{-1} with only a small decrease in τ_1 and τ_2 values (Table 1). Such effective fluorescence quenching by 7.5 μM of **1** is unlikely to be dynamic in nature. Instead ground state static quenching by extremely rapid exciton diffusion along the PPE-SO$_3^-$ chain to **1** that is bound onto the anionic polymer chain by electrostatic and/or $\pi-\pi$ interactions should be the main reason for the quenching. At 15 μM concentration of **1**, τ_1 and τ_2 are found to decrease significantly, and K_{SV} is increased to a great extent to 1.01 × 10^6 M^{-1} s^{-1}. These suggest that in addition to ground state static quenching, another quenching pathway may be operative which becomes more important at 15 μM of **1**. As there is a growth of the ^{3}MMLCT emission of **1** centered at ~795 nm, resulting from the self-assembly and formation of polymer–metal

18778

dx.doi.org/10.1021/ja205996e |*J. Am. Chem. Soc.* 2011, 133, 18775–18784
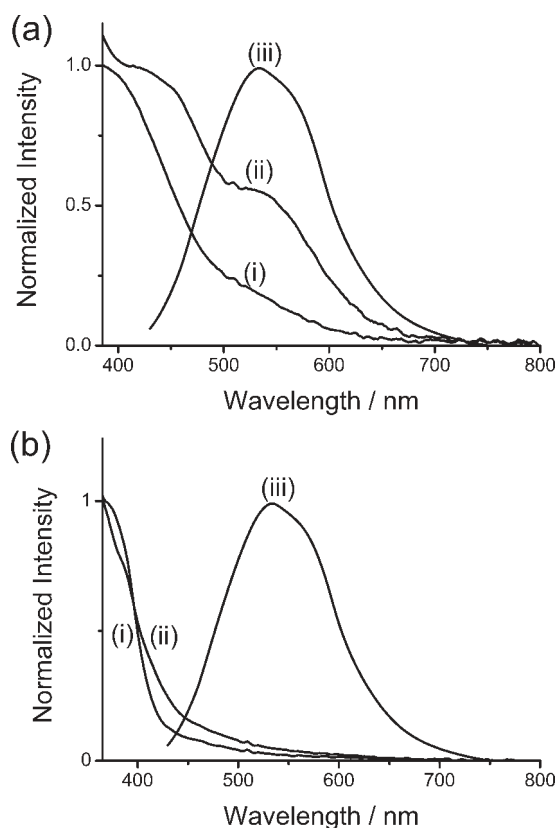
Figure 5. Normalized electronic absorption spectra of **1** and **2** and the emission spectrum of PPE-SO$_3^-$ showing the spectral overlap between the electronic absorption spectra of **1** and **2** with the emission spectrum of PPE-SO$_3^-$. (a) The electronic absorption spectra of **1** (i) in the absence of polyelectrolyte and (ii) in the presence of poly(sodium p-styrenesulfonate) with 45 μM sulfonate concentration were normalized at 396 and 409 nm respectively, while the emission spectrum of PPE-SO$_3^-$ with 45 μM of PE-SO$_3^-$ was normalized at 535 nm. (b) The electronic absorption spectra of **2** (i) in the absence of polyelectrolyte and (ii) in the presence of poly(sodium p-styrenesulfonate) with 45 μM sulfonate concentration were normalized at 368 and 366 nm respectively, while the emission spectrum of PPE-SO$_3^-$ with 45 μM of PE-SO$_3^-$ was normalized at 535 nm. All the spectra were recorded in an aqueous buffer solution (30 mM Tris-HCl, 30 mM NaCl, pH 9.0). Electronic absorption spectra of the aggregated **1** and **2** were recorded using poly(sodium p-styrenesulfonate) instead of PPE-SO$_3^-$, in order to prevent the interference of the electronic absorption of **1** and **2** by the conjugated polymer.

complex aggregates via Pt···Pt, electrostatic and/or $\pi-\pi$ interactions, which has been further supported by RLS experiments (Figure S2 in SI), a better spectral overlap between the emission spectrum of PPE-SO$_3^-$ and the absorption spectrum of the aggregated **1** on the polymer chains when compared to that between the emission spectrum of PPE-SO$_3^-$ and the absorption spectrum of non-aggregated **1** (Figure 5a) is anticipated, and thus, it is likely that FRET would occur. In addition, the formation of the polymer—metal complex aggregates could increase the chance of interchain diffusion of excitons from PPE-SO$_3^-$ to complex **1**, leading to the obvious decrease in τ_1 and τ_2 at 15 μM of **1** and favoring the FRET from PPE-SO$_3^-$ to the aggregated **1** on the polymer chains, so that the emission quenching of PPE-SO$_3^-$ is more effective with an increased K_{SV} value. At higher concentration of **1** (from 22.5 to 45 μM),
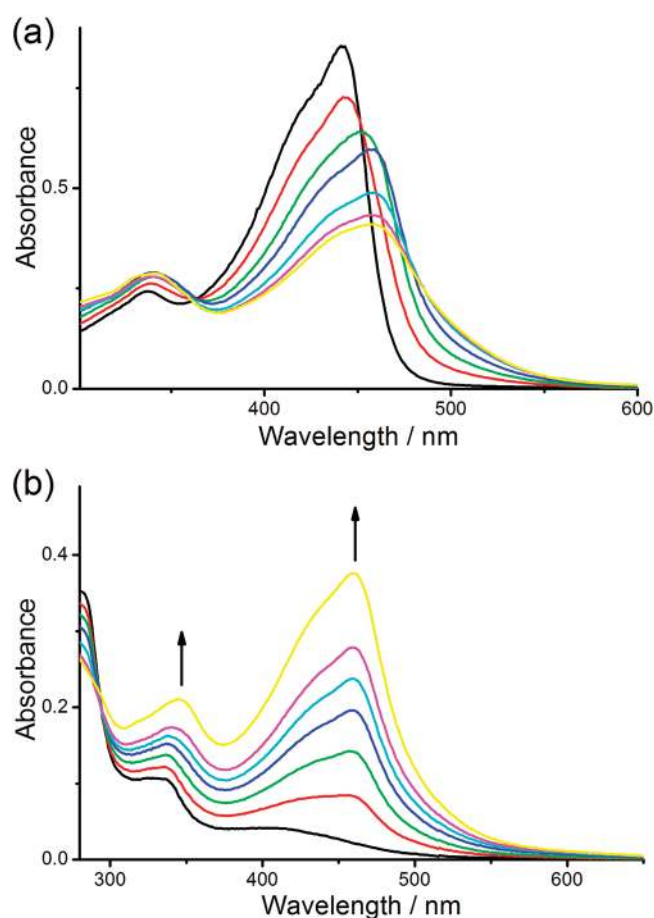
Figure 6. (a) Electronic absorption spectral changes of PPE-SO$_3^-$ in an aqueous buffer solution (30 mM Tris-HCl, 30 mM NaCl, pH 9.0) with an increasing concentration of **2**. Concentration of PE-SO$_3^-$ and **2** were 45 μM and (black) 0 μM, (red) 7.5 μM, (green) 15 μM, (blue) 22.5 μM, (cyan) 30 μM, (magenta) 37.5 μM and (yellow) 45 μM, respectively. (b) Electronic absorption spectral changes of **2** in an aqueous buffer solution (30 mM Tris-HCl, 30 mM NaCl, pH 9.0) with an increasing concentration of PPE-SO$_3^-$. Concentration of **2** and PE-SO$_3^-$ were 45 μM and (black) 0 μM, (red) 7.5 μM, (green) 15 μM, (blue) 22.5 μM, (cyan) 30 μM, (magenta) 37.5 μM and (yellow) 45 μM, respectively.

a further drop in the intensity of PPE-SO$_3^-$ fluorescence has been observed, as expected of a quenching process. However, a further increase in K_{SV} and a growth of the ^{3}MMLCT emission in the steady-state emission measurement as well as a decrease in τ_1 and τ_2 in the time-resolved emission measurement have been observed, indicating that the quenching is not simply due to an increase in the quencher concentration but probably also due to an increasing aggregation of **1** onto the PPE-SO$_3^-$ chains. The increased aggregation of **1** would enhance the formation of polymer—metal complex (PPE-SO$_3^-$—**1**) aggregates through stronger electrostatic and $\pi-\pi$ interactions with PPE-SO$_3^-$ at higher concentration of **1** as illustrated in the RLS spectra (Figure S2 in SI). This would lead to an increase in the absorbance of the low-energy MMLCT absorption band of **1**, resulting in a better spectral overlap between the PPE-SO$_3^-$ donor and the aggregate of **1** acceptor, which favor the FRET process.

Similarly, the emission spectral changes of the converse titration of **1** with PPE-SO$_3^-$ (Figure S1 in SI) can be explained by the polymer—metal complex aggregate formation and the
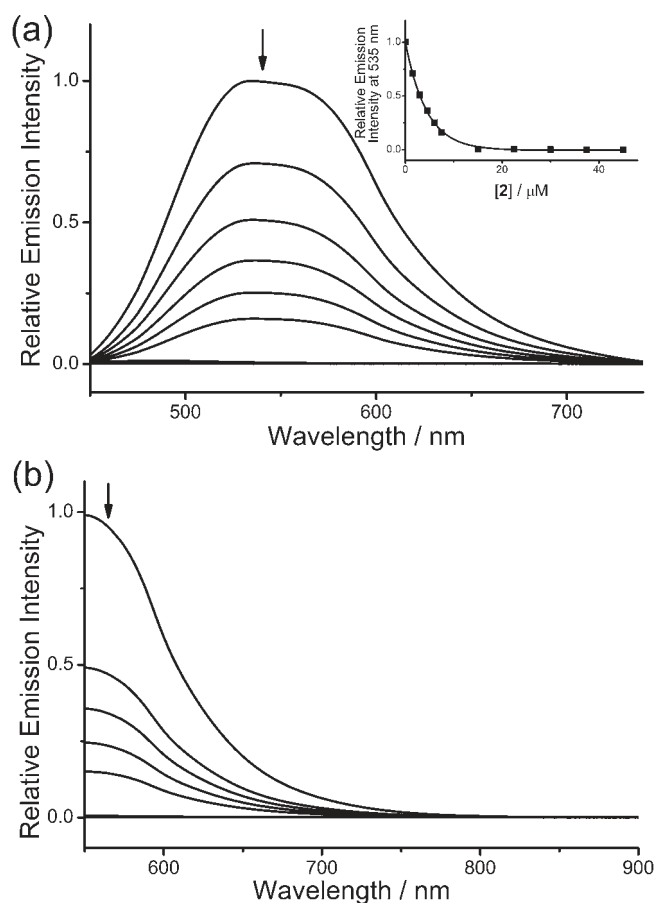
Figure 7. Emission spectral changes of PPE-SO$_3^-$ in aqueous buffer solution (30 mM Tris-HCl, 30 mM NaCl, pH 9.0) with an increasing concentration of **2** in the range of (a) 450−740 nm and (b) 550−900 nm. Concentration of PE-SO$_3^-$ was 45 μM. Inset: Plot of relative emission intensity at 535 nm versus concentration of **2**.

FRET from PPE-SO$_3^-$ to 1. At low concentrations of PE-SO$_3^-$, addition of PPE-SO$_3^-$ would increase the aggregation of **1** onto the polymer, leading to a better spectral overlap and FRET from PPE-SO$_3^-$ to the aggregated **1**. As a result, there is a growth of the ^{3}MMLCT emission of **1** with no observable PPE-SO$_3^-$ fluorescence. On the other hand, at high concentrations of PE-SO$_3^-$, further addition of PPE-SO$_3^-$ would not increase the formation of polymer−metal complex aggregates as **1** has already been bound to the polymer. Instead, the excess PPE-SO$_3^-$ added might lead to a "dilution" of the negative charges and an increase in the hydrophobic phenyl rings, causing complex molecules of **1** to redistribute themselves among different PPE-SO$_3^-$ chains, leading to a reduced self-aggregation of **1**, similar to the study of **1** with polyelectrolytes.[4d] Therefore, a decrease in FRET with a drop in ^{3}MMLCT emission and a growth of PPE-SO$_3^-$ fluorescence is observed.

The electronic absorption spectral changes of [Pt(tpy)-(C≡CCH$_2$NMe$_3$)](OTf)$_2$ (**2**) and PPE-SO$_3^-$ (Scheme 1) in the aqueous buffer solution (30 mM Tris-HCl, 30 mM NaCl, pH 9.0) are shown in Figure 6. Similar to the spectral changes of PPE-SO$_3^-$ with **1**, red shifts of the absorption bands centered at 336 and 435 nm to 342 and 459 nm, respectively, with increasing concentration of **2** have been observed, while converse titration of **2** with PPE-SO$_3^-$ would lead to the growth of the absorptions

at ∼333 and 405 nm with red shifts to ∼345 and 469 nm, respectively. Both observations suggest a conformational change of the PPE-SO$_3^-$ in the aqueous buffer solution.[7k] As **2** has been found to undergo aggregation in the presence of polyelectrolytes similar to that of **1**,[4d] together with the growth of the maximum in the RLS spectra (Figure S3 in SI), the conformational change is similarly ascribed to the formation of polymer−metal complex aggregates with Pt···Pt, electrostatic and $\pi-\pi$ interactions. For the emission spectra of PPE-SO$_3^-$ excited at the isosbestic wavelength of 362 nm in the presence of different concentrations of **2** (Figure 7), the $^1\pi-\pi^*$ fluorescence of PPE-SO$_3^-$ at 535 nm has been found to be quenched significantly by **2**, but there was no growth of NIR emission as observed in the study of PPE-SO$_3^-$ with **1**. The decrease in the emission at 535 nm can be similarly explained by the amplified quenching at low concentrations of **2** and the formation of polymer−metal complex aggregates at higher concentrations. The converse titration of **2** with PPE-SO$_3^-$ was also found to show no significant growth of the emission in the NIR region (Figure S4 in SI). Interestingly, although **2** can undergo aggregation in the presence of polyelectrolytes such as poly(sodium *p*-styrenesulfonate), its ^{3}MMLCT emission is centered at ∼668 nm (Figure S5 in SI).[4] As the electronic absorption spectra of both the non-aggregated and aggregated **2** had poor spectral overlap with the emission of PPE-SO$_3^-$ (Figure 5b), it is unlikely that efficient FRET would occur from PPE-SO$_3^-$ to **2**. Thus, the growth of the emission band at 795 nm in the study of **1** and PPE-SO$_3^-$ is a result of the FRET process from PPE-SO$_3^-$ to **1**, and not a result of the direct excitation of the aggregated **1** on the anionic PPE-SO$_3^-$ chain.
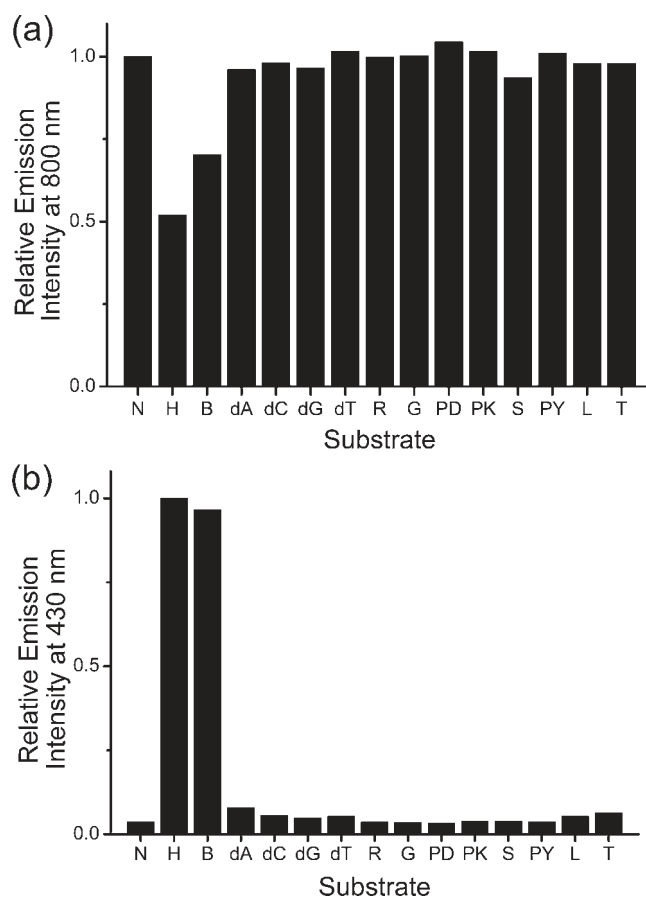
As the polymer−platinum(II) complex (PPE-SO$_3^-$−**1**) ensemble shows FRET interaction and NIR emission which are both attractive features for detection of biological samples, this has prompted us to explore a "proof-of-principle" concept for the sensing of HSA. Since cationic platinum(II) complexes have been found to undergo aggregation in the presence of anionic polyelectrolytes through electrostatic interaction,[4] the use of the two-component ensemble for sensing studies in aqueous buffer solution at pH 9 will be affected by anionic biological substrates (Figure S6 in SI). Therefore, the sensing ensemble has been employed to operate at pH 3 aqueous buffer solution (40 mM citric acid, 60 mM NaCl, and 21 mM NaOH) where most of the biological samples have been turned into their neutral or cationic form, minimizing their interference in sensing HSA, while there is still FRET between PPE-SO$_3^-$ and **1**. It is interesting to note that the electronic absorption spectra, emission spectra, and time-resolved emission measurement of PPE-SO$_3^-$ and **1** in pH 3 aqueous buffer solution are found to be similar to those in pH 9 buffer solution (Figures S7, S8, and S9 and Table S1 in SI). This is understandable as the sulfonate groups in PPE-SO$_3^-$ are strongly acidic (pK_a = −2.6) and will remain negatively charged at pH 3,[18] resulting in electrostatic interaction with **1**. In addition, Pt···Pt and $\pi-\pi$ interactions would also likely be involved in the formation of polymer−metal complex aggregates, favoring FRET from PPE-SO$_3^-$ to **1**.

The emission spectra of PPE-SO$_3^-$ and **1** in pH 3 aqueous buffer solution (40 mM citric acid, 60 mM NaCl and 21 mM NaOH), with λ_{ex} = 362 nm, are shown in Figure S10 and S11 in SI. Upon the addition of HSA which was freshly incubated in pH 6.8 aqueous buffer solution (50 mM KH$_2$PO$_4$), there is a drop in the emission band at 800 nm, with a concomitant growth of the emissions centered at 430 and 480 nm. The emission centered at 800 nm, which is tentatively assigned as ^{3}MMLCT emission with
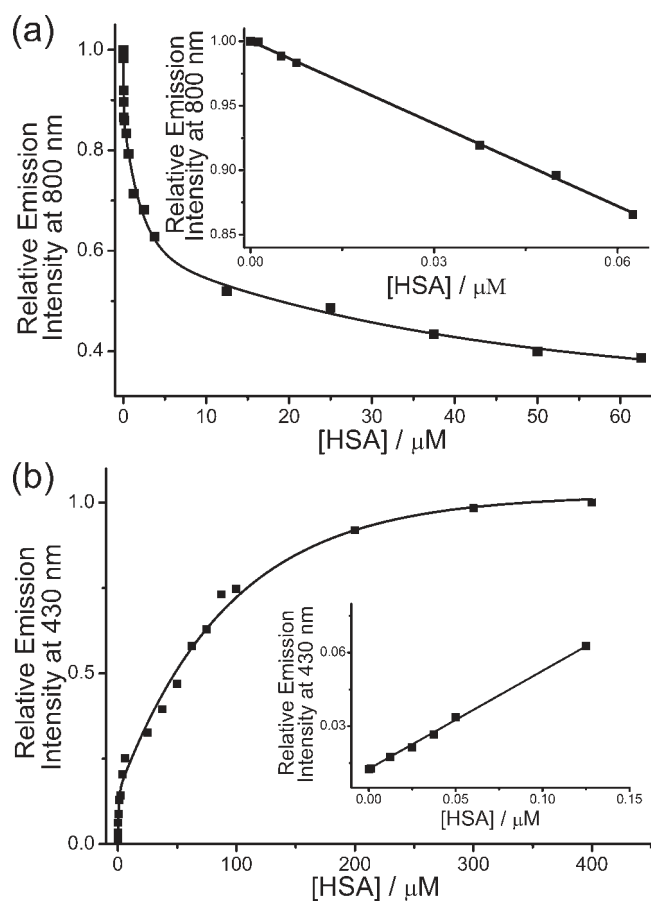
Figure 8. Relative emission intensity of PPE-SO$_3^-$ and **1** at (a) 800 nm and (b) 430 nm versus concentration of HSA. Concentration of PE-SO$_3^-$ and **1** in the final solution mixture were both 45 μM. Inset: Plot of relative emission intensity at 800 and 430 nm versus concentration of HSA, showing the linear relationships between the relative emission intensities and the concentration of HSA at low concentration.
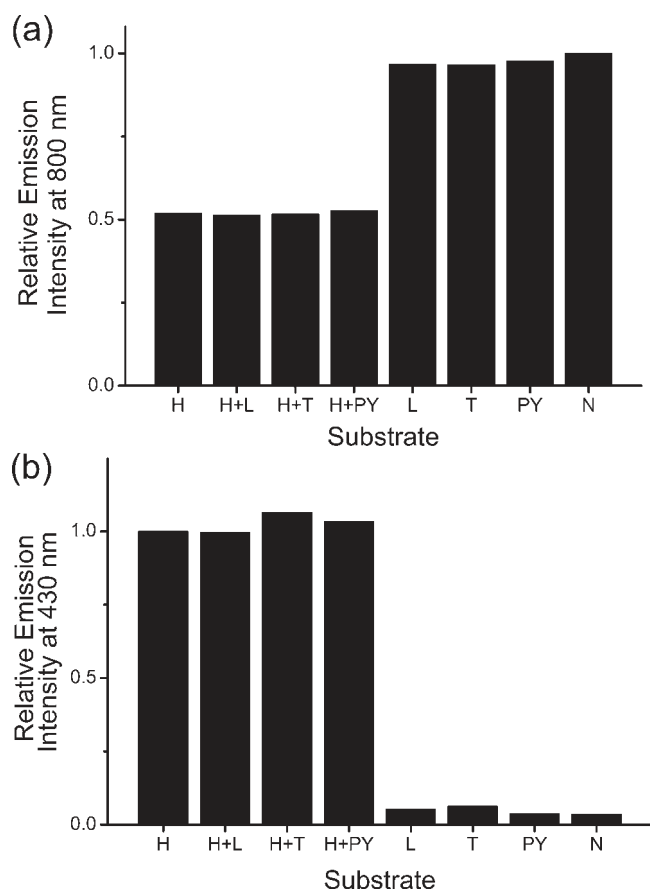

Figure 9. Relative emission intensity of PPE-SO$_3^-$ and **1** at (a) 800 nm and (b) 430 nm in the presence of different substrates. Substrate tested: N: no substrate added, H: 12.5 μM HSA, B: 12.5 μM bovine serum albumin, dA: 12.5 μM poly(dA)$_{25}$, dC: 12.5 μM poly(dC)$_{25}$, dG: 12.5 μM poly(dG)$_{25}$, dT: 12.5 μM poly(dT)$_{25}$, R: 1.25 mM arginine, G: 1.25 mM glycine, PD: 12.5 μM poly(aspartic acid), PK: 12.5 μM poly(lysine bromide), S: 1.25 mM spermine, PY: 12.5 μM poly-(tyrosine), L: 12.5 μM lysozyme, T: 12.5 μM trypsin. Concentration of PE-SO$_3^-$ and **1** in the final solution mixture were both 45 μM.

reference to previous spectroscopic work on complex **1**,[4d,g] should be due to the FRET from PPE-SO$_3^-$ to the aggregated **1** on the polymer similar to the study in pH 9 buffer solution. The decrease in ^{3}MMLCT emission upon addition of HSA suggests that a decrease in FRET has occurred. For the emissions centered at 430 and 480 nm, they should be originated from the recovery of the emission of PPE-SO$_3^-$ but are blue-shifted compared to the $^1\pi-\pi^*$ fluorescence of PPE-SO$_3^-$ in aqueous solution ($\sim$550 nm). Thus, it is likely that PPE-SO$_3^-$ is in a less aggregated state or is located in a more hydrophobic environment[9b] in the presence of HSA. As it has been reported that bovine serum albumin (BSA) can complex to CPEs by the hydrophobic patches,[11b] PPE-SO$_3^-$ is probably bound to HSA by electrostatic and hydrophobic interactions, leading to the deaggregation of the polymer−metal complex aggregates and the decrease in FRET from PPE-SO$_3^-$ to **1**, as revealed by the increase in τ_1 and τ_2 values upon the addition of HSA (Figure S12 in SI). These in turn would result in the higher-energy $^1\pi-\pi^*$ fluorescence of the less aggregated PPE-SO$_3^-$ in a more hydrophobic environment after binding with HSA, when compared to the emission of the aggregated PPE-SO$_3^-$ in aqueous solution. The electrostatic interaction between PPE-SO$_3^-$ and HSA could not be ignored because HSA is highly positively charged at pH 3 and it contains 23 Arg residues in its monomeric

state[19] which would have very strong electrostatic interaction as well as hydrogen bonding with the sulfonate groups on PPE-SO$_3^-$.[18,20] With an increasing concentration of HSA, more PPE-SO$_3^-$ molecules would be bound to HSA and more polymer−metal complex aggregates would be destroyed, leading to a drop of the ^{3}MMLCT emission intensity at 800 nm to only 40% of that without HSA, and a 48-fold increase of the $^1\pi-\pi^*$ fluorescence of PPE-SO$_3^-$ centered at 430 nm at 400 μM of HSA. This two-component ensemble has a high sensitivity in the detection of HSA as the spectral changes are detectable even at 1.25 nM HSA. In addition, the relative emission intensity at 800 nm is found to show a linear relationship with [HSA] from 1.25 to 62.5 nM, and similarly the relative emission intensity at 430 nm is found to vary linearly with [HSA] from 1.25 to 125 nM (Figure 8).

As the fluorescence of CPEs has been reported to be affected by various polyelectrolytes,[9b,11] the selectivity of the two-component ensemble toward HSA has also been probed (Figure 9). Since the polymer−metal complex aggregates are formed by electrostatic and $\pi-\pi$ interactions between PPE-SO$_3^-$ and **1** as well as by Pt···Pt interaction among **1**, highly positively charged

Figure 10. Relative emission intensity of PPE-SO$_3^-$ and **1** at (a) 800 nm and (b) 430 nm in the presence of: H: 12.5 μM HSA, H+L: 12.5 μM HSA and 12.5 μM lysozyme, H+T: 12.5 μM HSA and 12.5 μM trypsin, H+PY: 12.5 μM HSA and 12.5 μM poly(tyrosine), L: 12.5 μM lysozyme, T: 12.5 μM trypsin, PY: 12.5 μM poly(tyrosine); N: No substrate added. Concentration of PE-SO$_3^-$ and **1** in the final solution mixture were both 45 μM.

poly(lysine bromide), and spermine, singly positively charged poly(aspartic acid) and glycine molecules, and neutral poly-(tyrosine) and poly(nucleotides)[21] at pH 3 have been tested. Interestingly, no significant change in the emission intensity of the ensemble has been observed, suggesting that the polymer–metal complex aggregates cannot be significantly destroyed by electrostatic or hydrophobic interactions alone. Although the guanidinium moieties of arginine residues have been reported to show strong electrostatic interactions and hydrogen bonding with the sulfonate groups of PPE-SO$_3^-$,[18,20] they still could not destroy the strong polymer–metal complex aggregates and would not interfere with the detection of HSA. For large proteins such as lysozyme and trypsin, significant spectral changes of the ensemble have also not been observed. This may be explained by their weaker interactions with the polymer–metal complex aggregates than that of HSA, as both of them contain only six Arg residues and do not have as many hydrophobic patches as HSA.[22] Further studies on the detection of HSA in the presence of trypsin, lysozyme, and poly(tyrosine) show that there is only a small discrepancy in emission intensities at 430 and 800 nm as compared to the emission intensity in the presence of HSA alone (Figure 10). As a result, this two-component polymer–metal complex ensemble is found to show a good selectivity toward the

detection of HSA, which is not observed in other fluorescence sensors of HSA,[16b−e] as well as in the study of CPEs as the emission of CPEs are usually found to be interfered by various polyelectrolytes.[9e,11] This may probably be due to the fact that strong polymer–metal complex aggregates are formed through Pt···Pt, electrostatic and π–π interactions and HSA is one of the proteins that is rich in arginine residues and hydrophobic patches.[19]

Attempts to explore the applicability of this system close to the physiological pH have also been explored. The detection of HSA by the ensemble solution at pHs 4, 5, and 6 using succinic acid/potassium hydroxide buffer solution with 0.01 M ionic strength[23] has been tested. The emission spectral changes in the visible and NIR region are found to be less significant at pH 5 compared to the changes at pH 4, and are even smaller at pH 6 (Figure S13 in SI). This can be explained by the pI value of HSA which is 4.7.[19] HSA is positively charged at pH 4 so that there would be strong electrostatic and π–π interactions with PPE-SO$_3^-$, leading to deaggregation of the polymer–metal complex aggregates with significant spectral changes in the visible and NIR region. On the other hand, HSA is almost neutral at pH 5 so that its interaction with PPE-SO$_3^-$ would be weak, with little deaggregation of the polymer–metal complex aggregates, resulting in smaller spectral changes. At pH 6, HSA is negatively charged, so that its interaction with the aggregates would be quite different from that at pH 4 and 5. As there are small changes in the NIR region, the negatively charged HSA would probably be bound with the positively charged complex **1** through electrostatic interactions and PPE-SO$_3^-$ through the hydrophobic patches as suggested from the blue shift of the PPE-SO$_3^-$ fluorescence. As a result, complex **1** would form aggregates on HSA and the drop in ^{3}MMLCT emission would be smaller when compared to the deaggregation of **1** that would occur upon the binding of PPE-SO$_3^-$ with HSA at pHs 4 and 5.

In summary, the sensing of HSA at lower pH is found to have more significant changes in the visible and NIR region as well as less interference from other substrates. Therefore, the ensemble in pH 3 buffer solution (40 mM citric acid, 60 mM NaCl, and 21 mM NaOH) should be the optimum condition for the sensing of HSA among those being tested.

■ CONCLUSION

In the present study, a platinum(II) complex, **1**, has been shown to assemble onto the anionic conjugated polymer, PPE-SO$_3^-$, through Pt···Pt, electrostatic, and π–π interactions, leading to the formation of polymer–metal complex aggregates and FRET with a growth of ^{3}MMLCT emission in the NIR region. This two-component ensemble has been demonstrated for the label-free spectroscopic detection of HSA with high selectivity and sensitivity by monitoring the deaggregation of polymer–metal complex aggregates with Pt···Pt interaction and the decrease in FRET, which are reflected from the ^{3}MMLCT NIR emission and $^1\pi$–π^* fluorescence of PPE-SO$_3^-$.

■ EXPERIMENTAL SECTION

Materials and Reagents. Human serum albumin (HSA), bovine serum albumin (BSA), lysozyme, trypsin, poly(L-lysine bromide) (M_w = 15,000), poly(aspartic acid) (M_w = 10,300), poly(L-arginine hydrochloride) (M_w = 35,500), poly(tyrosine) (M_w = 10,000−40,000), and spermine were purchased from Sigma-Aldrich. Poly(nucleotides) were obtained from Sigma-Proligo (St. Louis, MO). Poly(sodium

p-styrenesulfonate) ($M_w \approx 70{,}000$) was purchased from Acros. All other reagents were of analytical grade and were used without further purification. The reactions were performed under an inert atmosphere of nitrogen unless specified otherwise.

Physical Measurements and Instrumentation. ^{1}H NMR spectra were recorded with a Bruker AVANCE 400 (400 MHz) Fourier transform NMR spectrometer at ambient temperature with tetramethyl-silane (Me$_4$Si) as an internal reference. Positive ion FAB or EI mass spectra were recorded on a Thermo Scientific DFS high-resolution magnetic sector mass spectrometer. Elemental analyses for the metal complexes were performed on the Carlo Erba 1106 elemental analyzer at the Institute of Chemistry, Chinese Academy of Sciences, Beijing, China. IR spectra of the solid samples were obtained as Nujol mulls on KBr disks on a Bio-Rad FTS-7 Fourier transform infrared spectrophotometer ($4000-400$ cm^{-1}). UV–vis absorption spectra were recorded on a Cary 50 (Varian) spectrophotometer equipped with a Xenon flash lamp. Steady state emission spectra were recorded using a Spex Fluorolog-3 model FL3-211 fluorescence spectrofluorometer equipped with a R2658P PMT detector. Time-resolved fluorescence spectra were recorded with a Horiba Jobin Yvon FluoroCube based on a time-correlated single-photon counting method, using a nanoLED with peak wavelength and pulse duration equal to 371 nm and <200 ps, respectively, as the excitation source. Unless specified otherwise, the emission spectra were corrected for PMT response. Resonance light-scattering (RLS) experiments were performed on Spex Fluorolog-3 model FL3-211 fluorescence spectrofluorometer with a Xenon flash lamp using a right-angle geometry to a R2658P PMT detector. The excitation and emission monochromator wavelengths were coupled and adjusted to scan simultaneously through the range of $350-600$ nm.

Synthesis of Complexes 1 and 2. The ligands [H−C≡CC$_6$H$_4$−CH$_2$NMe$_3$-4](OTf) and [H−C≡CCH$_2$NMe$_3$](OTf), and complexes **1** and **2** were synthesized as reported previously.[4d,g]

Synthesis of PPE-SO$_3^-$Na$^+$. The polymer was synthesized according to the method reported in the literature.[7d,f,g] 3,3′-[(2,5-Diiodo-1,4-phenylene)bis(oxy)]bis-1-propanesulfonate in sodium salt (504.4 mg, 0.776 mmol), 1,4-diethynylbenzene (94.5 mg, 0.75 mmol), Pd(PPh$_3$)$_4$ (26.0 mg, 22.5 μmol), and CuI (5 mg, 22.5 μmol) were deoxygenated by vacuum-argon cycling and reacted in a mixture of DMF, H$_2$O, and diisopropylamine at 60 °C with stirring under a positive pressure of argon for 14 h. The product was purified by precipitation in methanol−acetone−diethyl ether mixture, dialysis against water using a 6−8 kD MWCO cellulose membrane and precipitation in a large volume of methanol−acetone−diethyl ether mixture. The product was collected as yellow fibers. Its purity was confirmed by ^{1}H NMR, and the molecular weight was estimated to be 150 kD on the basis of its ultrafiltration properties. Yield = 200 mg (51.2%). ^{1}H NMR (400 MHz, DMSO-d_6, 353 K): δ = 2.12 (br, 4H), 2.71 (br, 4H), 4.14 (br, 4H), 7.17 (br, 2H), 7.76 (br, 4H).

Methods in the Sensing Studies. HSA and all the other substrates tested were first incubated in pH 6.8 aqueous buffer solution (50 mM KH$_2$PO$_4$) at 37 °C for 30 min. Then 20 μL of solution was transferred to 480 μL of solution mixture of the ensemble in pH 3 aqueous buffer solution (40 mM citric acid, 60 mM NaCl, and 21 mM NaOH), and the emission spectra were recorded by excitation at 362 nm. The concentration of sulfonate groups in PPE-SO$_3^-$ (PE-SO$_3^-$) and **1** in the final solution mixture were both 45 μM.

■ ASSOCIATED CONTENT

ⓈSupporting Information. Emission spectral changes of **1** and **2** with different concentrations of PPE-SO$_3^-$. RLS spectra of PPE-SO$_3^-$ with different concentrations of **1** and **2**. Emission spectrum of **2** in the presence of polyelectrolyte. Emission spectra of PPE-SO$_3^-$ and **1** in pH 9 buffer solution in the presence of polyelectrolytes. Electronic absorption spectra, steady-state emission spectra, time-resolved emission spectra and table summarizing the parameters obtained from steady-state emission spectra and time-resolved emission spectra of PPE-SO$_3^-$ and **1** in pH 3 buffer solution. Emission spectra of PPE-SO$_3^-$ and **1** with different concentrations of HSA. Time-resolved emission spectra of PPE-SO$_3^-$ and **1** in the presence of HSA. Relative emission intensity of the ensemble at pHs 4, 5, and 6 (succinic acid/potassium hydroxide, 0.01 M ionic strength) with different concentrations of HSA. This material is available free of charge via the Internet at http://pubs.acs.org.

■ AUTHOR INFORMATION

Corresponding Author
wwyam@hku.hk

■ ACKNOWLEDGMENT

■ REFERENCES

(1) (a) Osborn, R. S.; Rogers, D. *J. Chem. Soc., Dalton Trans.* **1974**, 1002. (b) Jennette, K. W.; Gill, J. T.; Sadownick, J. A.; Lippard, S. J. *J. Am. Chem. Soc.* **1976**, *98*, 6159. (c) Miskowski, V. M.; Houlding, V. H. *Inorg. Chem.* **1991**, *30*, 4446. (d) Houlding, V. H.; Miskowski, V. M. *Coord. Chem. Rev.* **1991**, *111*, 145. (e) Büchner, R.; Cunningham, C. T.; Field, J. S.; Haines, R. J.; McMillin, D. R.; Summerton, G. C. *J. Chem. Soc., Dalton Trans.* **1999**, 711. (f) Yam, V. W. W.; Wong, K. M. C.; Zhu, N. *J. Am. Chem. Soc.* **2002**, *124*, 6506.

(2) (a) Yam, V. W. W.; Tang, R. P. L; Wong, K. M. C.; Cheung, K. K. *Organometallics* **2001**, *20*, 4476. (b) Goshe, A. J.; Steele, I. M.; Bosnich, B. *J. Am. Chem. Soc.* **2003**, *125*, 444. (c) Büchner, R.; Field, J. S.; Haines, R. J.; Cunningham, C. T.; McMillin, D. R. *Inorg. Chem.* **1997**, *36*, 3952. (d) Wadas, T. J.; Wang, Q. M.; Kim, Y. J.; Flaschenreim, C.; Blanton, T. N.; Eisenberg, R. *J. Am. Chem. Soc.* **2004**, *126*, 16841. (e) Herber, R. H.; Croft, M.; Coyer, M. J.; Bilash, B.; Sahiner, A. *Inorg. Chem.* **1994**, *33*, 2422. (f) Connick, W. B.; Henling, L. M.; Marsh, R. E.; Gray, H. B. *Inorg. Chem.* **1996**, *35*, 6261. (g) Connick, W. B.; Marsh, R. E.; Schaefer, W. P.; Gray, H. B. *Inorg. Chem.* **1997**, *36*, 913.

(3) (a) Wong, K. M. C.; Tang, W. S.; Lu, X. X.; Zhu, N.; Yam, V. W. W. *Inorg. Chem.* **2005**, *44*, 1492. (b) Tang, W. S.; Lu, X. X.; Wong, K. M. C.; Yam, V. W. W. *J. Mater. Chem.* **2005**, *15*, 2714. (c) Lo, H. S.; Yip, S. K.; Wong, K. M. C.; Zhu, N.; Yam, V. W. W. *Organometallics* **2006**, *25*, 3537. (d) Lo, H. S.; Yip, S. K.; Zhu, N.; Yam, V. W. W. *Dalton Trans.* **2007**, 4386.

(4) (a) Yu, C.; Wong, K. M. C.; Chan, K. H. Y.; Yam, V. W. W. *Angew. Chem., Int. Ed.* **2005**, *44*, 791. (b) Yam, V. W. W.; Chan, K. H. Y.; Wong, K. M. C.; Chu, B. W. K. *Angew. Chem., Int. Ed.* **2006**, *45*, 6169. (c) Yu, C.; Chan, K. H. Y.; Wong, K. M. C.; Yam, V. W. W. *Proc. Natl. Acad. Sci. U. S. A.* **2006**, *103*, 19652. (d) Yu, C.; Chan, K. H. Y.; Wong, K. M. C.; Yam, V. W. W. *Chem.—Eur. J.* **2008**, *14*, 4577. (e) Yu, C.; Chan, K. H. Y.; Wong, K. M. C.; Yam, V. W. W. *Chem. Commun.* **2009**, 3756. (f) Yeung, M. C. L.; Wong, K. M. C.; Tsang, Y. K. T.; Yam, V. W. W. *Chem. Commun.* **2010**, *46*, 7709. (g) Chung, C. Y. S.; Chan, K. H. Y.; Yam, V. W. W. *Chem. Commun.* **2011**, *47*, 2000.

(5) (a) Yip, H. K.; Che, C. M.; Zhou, C. M.; Mak, T. C. W. *J. Chem. Soc., Chem. Commun.* **1992**, 1369. (b) Bailey, J. A.; Miskowski, V. M.; Gray, H. B. *Inorg. Chem.* **1993**, *32*, 369. (c) Hill, M. G.; Bailey, J. A.; Miskowski, V. M.; Gray, H. B. *Inorg. Chem.* **1996**, *35*, 4585.

(6) (a) Camerel, F.; Ziessel, R.; Donnio, B.; Bourgogne, C.; Guillon, D.; Schmutz, M.; Iacovita, C.; Bucher, J. P. *Angew. Chem., Int. Ed.* **2007**, *46*, 2659. (b) Yuen, M. Y.; Roy, V. A. L.; Lu, W.; Kui, S. C. F.; Tong, G. S. M.; So, M. H.; Chui, S. S. Y.; Muccini, M.; Ning, J. Q.; Xu, S. J.; Che, C. M. *Angew. Chem., Int. Ed.* **2008**, *47*, 9895.

(7) (a) Zhou, Q.; Swager, M. *J. Am. Chem. Soc.* **1995**, *117*, 12593. (b) Miteva, T.; Palmer, L.; Kloppenburg, L.; Neher, D.; Bunz, U. H. F. *Macromolecules* **2000**, *33*, 652. (c) Kim, J.; Swager, T. M. *Science* **2001**, *411*, 1030. (d) Tan, C.; Pinto, M. R.; Schanze, K. S. *Chem. Commun.* **2002**, 446. (e) Kushon, S. A.; Ley, K. D.; Bradford, K.; Jones, R. M.; McBranch, D.; Whitten, D. *Langmuir* **2002**, *18*, 7274. (f) Pinto, M. R.; Kristal, B. M.; Schanze, K. S. *Langmuir* **2003**, *19*, 6523. (g) Kushon, S. A.; Bradford, K.; Marin, V.; Suhrada, C.; Armitage, B. A.; McBranch, D.; Whitten, D. *Langmuir* **2003**, *19*, 6456. (h) Pinto, M. R.; Schanze, K. S. *Proc. Natl. Acad. Sci. U. S. A.* **2004**, *20*, 7505. (i) Kumaraswamy, S.; Bergstedt, T.; Shi, X.; Rininsland, F.; Kushon, S.; Xia, W.; Ley, K.; Achyuthan, K.; McBranch, D.; Whitten, D. *Proc. Natl. Acad. Sci. U. S. A.* **2004**, *20*, 7511. (j) Rininsland, F.; Xia, W.; Wittenburg, S.; Shi, X.; Stankewicz, C.; Achyuthan, K.; McBranch, D.; Whitten, D. *Proc. Natl. Acad. Sci. U. S. A.* **2004**, *43*, 15295. (k) Tan, C.; Atas, E.; Müller, J. G.; Pinto, M. R.; Kleiman, V. D.; Schanze, K. S. *J. Am. Chem. Soc.* **2004**, *126*, 13685. (l) Fan, L. J.; Jones, W. E., Jr. *J. Am. Chem. Soc.* **2006**, *128*, 6784. (m) Liu, Y.; Schanze, K. S. *Anal. Chem.* **2009**, *81*, 231. (n) Ding, L.; Chi, E. Y.; Schanze, K. S.; Lopez, G. P.; Whitten, D. *Langmuir* **2010**, *8*, 5544.

(8) (a) Harrison, B. S.; Ramey, M. B.; Reynolds, J. R.; Schanze, K. S. *J. Am. Chem. Soc.* **2000**, *122*, 8561. (b) Gaylord, B. S.; Heeger, A. J.; Bazan, G. C. *Proc. Natl. Acad. Sci. U. S. A.* **2002**, *17*, 10954. (c) Gaylord, B. S.; Heeger, A. J.; Bazan, G. C. *J. Am. Chem. Soc.* **2003**, *125*, 896.

(9) (a) Chen, L.; McBranch, D. W.; Wang, H. L.; Helgeson, R.; Wudl, F.; Whitten, D. *Proc. Natl. Acad. Sci. U. S. A.* **1999**, *22*, 12287. (b) Chen, L.; Xu, S.; McBranch, D.; Whitten, D. *J. Am. Chem. Soc.* **2000**, *122*, 9302. (c) Wang, J.; Wang, D.; Miller, E. K.; Moses, D.; Bazan, G. C.; Heeger, A. J. *Macromolecules* **2000**, *33*, 5153. (d) Fan, C.; Plaxco, K. W.; Heeger, A. J. *J. Am. Chem. Soc.* **2002**, *124*, 5642. (e) Zhao, D.; Du, J.; Chen, Y.; Ji, X; He, Z.; Chan, W. H. *Macromolecules* **2008**, *41*, 5373.

(10) Achyuthan, K. E.; Bergstedt, T. S.; Chen, L.; Jones, R. M.; Kumaraswamy, S.; Kushon, S. A.; Ley, K. D.; Lu, L.; McBranch, D.; Mukundan, H.; Rininsland, F.; Shi, X.; Xia, W.; Whitten, D. *J. Mater. Chem.* **2005**, *15*, 2648.

(11) (a) Lavigne, J. J.; Broughton, D. L.; Wilson, J. N.; Erdogan, B.; Bunz, U. H. F. *Macromolecules* **2003**, *36*, 7409. (b) Kim, I. B.; Dunkhorst, A.; Bunz, U. H. F. *Langmuir* **2005**, *21*, 7985.

(12) Förster, T. *Ann. Phys* **1948**, *2*, 55.

(13) (a) Peters, T., Jr. *Adv. Protein Chem.* **1985**, *37*, 161. (b) Carter, D. C.; Ho, J. X. *Adv. Protein Chem.* **1994**, *45*, 153. (c) Hu., Y. J.; Liu, Y.; Xiao, X. H. *Biomacromolecules* **2009**, *10*, 517.

(14) Murch, S. H.; Winyard, P. J. D.; Koletzko, S.; Wehner, B.; Cheema, H. A.; Risdon, R. A.; Phillips, A. D.; Meadows, N.; Klein, N. J.; Walker-Smith, J. A. *Lancet* **1996**, *347*, 1299.

(15) Hoogenberg, K.; Sluiter, W. J.; Dullaart, R. P. F *Acta Endrocrinol.* **1993**, *129*, 151.

(16) (a) Kessler, M. A.; Meinitzer, A.; Petek, W.; Wolfbeis, O. S. *Clin. Chem.* **1997**, *43*, 996. (b) Matulis, D.; Baumann, C. G.; Bloomfield, V. A.; Lovrien, R. E. *Biopolymers* **1999**, *49*, 451. (c) Suzuki, Y.; Yokoyama, K. *J. Am. Chem. Soc.* **2005**, *127*, 17799. (d) Ahn, Y. H.; Lee, J. S.; Chang, Y. T. *J. Comb. Chem.* **2008**, *10*, 377. (e) Hawe, A.; Sutter, M.; Jiskoot, W. *Pharm. Res.* **2008**, *25*, 1487.

(17) (a) Pasternack, R. F.; Bustamante, C.; Collings, P. J.; Glannetto, A.; Gibbs, E. J. *J. Am. Chem. Soc.* **1993**, *115*, 5393. (b) Pasternack, R. F.; Collings, P. J. *Science* **1995**, *269*, 935. (c) Arena, G.; Scolaro, M.; Pasternack, R. F.; Romeo, R. *Inorg. Chem.* **1995**, *34*, 2994.

(18) Schug, K. A.; Lindner, W. *Chem. Rev.* **2005**, *105*, 67.

(19) Peters, T., Jr. Serum Albumin. *The Plasma Proteins: Structure, Function, and Genetic Control*, 2nd ed.; Putnam, F. W., Ed.; Academic Press: New York, 1975; Vol. 1, pp 133−181.

(20) Friess, S. D.; Zenobi, R. *Mass Spectrom.* **2001**, *12*, 810.

(21) (a) Legault, P.; Pardi, A. *J. Am. Chem. Soc.* **1997**, *119*, 6261. (b) Verdolino, V.; Cammi, R.; Munk, B. H.; Schlegel, H. B. *J. Phys. Chem. B* **2008**, *112*, 16860.

(22) (a) Zhang, K.; Gao, R.; Zhang, H.; Cai, X.; Shen, C.; Wu, C.; Zhao, S.; Yu, L. *Biol. Reprod.* **2005**, *73*, 1064. (b) Travis, J.; Roberts, R. C. *Biochemistry* **1969**, *8*, 2884.

(23) Perrin, D. D. *Aust. J. Chem.* **1963**, *16*, 572.